with $d_A - d_B = 2 \times 10^{-5}$ Å. The topograph Fig. 1(c) was taken after an interval during which the crack was examined optically and immersion oil was allowed to run into it. It was found subsequently that a considerable relaxation of the displacements across the crack had taken place, as can be seen by comparing Figs. 1(c) and (b). It is clear that repetitive topography can reveal fringe movements of $^1/_5$ D or less on widely spaced fringes. (This measurement is facilitated by use of "landmarks" such as the images of strain-fields of inclusions which appear as the black "double-dots" scattered over the field of Fig. 1.) A fringe shift of $^1/_5$ D corresponds to a displacement of crystal A relative to crystal B of only 0.4 Å, in the case of the reflection of Figs. 1(b) and (c).

The fringes at this and other cracks exhibit the following characteristics, which are in accord both with the simple geometrical analysis given above and with expectations from the dynamical electron diffraction theory of moiré fringes[6,7] appropriately applied to the x-ray case.

1. The moiré fringe pattern in the reflection nh, nk, nl is geometrically similar to that in the reflection hkl, but $D(nh, nk, nl) = (1/n)/D(hkl)$. This is the unfailing diagnostic characteristic identifying moiré fringes.

2. Moiré fringe contrast is strongest when the component of **G** normal to the Ewald sphere is smallest. The fringes are then modulated with a depth periodicity of half the Pendellösung period[6,7] [this is seen well in the upper right-hand fringes in Fig. 1(a)]. When the component of **G** normal to the Ewald sphere is relatively large, so that coherent simultaneous reflection by crystals A and B no longer occurs, the moiré fringes disappear and only depth contours with the full Pendellösung periodicity appear, as they do in images of tapering crystals[8] and of low-angle boundaries.[9] Usually a complicated pattern of crossed moiré and depth contours appears.

3. The moiré pattern in general differs in reflections from different Bragg planes, because each reflection is sensitive to different components of the relative "rotation" and "compression" of the two crystals.

The clear visibility of moiré fringes formed by two parts of a crystal separated by a crack indicates the feasibility of observing moiré fringes over a large area where two perfect crystals are super-imposed. Moreover, if one crystal were attached to the moving member of an optical interferometer then the number of interplanar spacings contained in a standard light wavelength could be found by counting simultaneously the moving x-ray moiré and light interference fringes.

[1] On leave from Institute of Crystallography, Academy of Sciences of U.S.S.R., Moscow, U.S.S.R.

[2] H. Hashimoto and R. Uyeda, *Acta Cryst.* **10,** 143 (1957).
[3] G. A. Bassett, J. W. Menter and D. W. Pashley, *Proc. Roy. Soc.* **A246,** 345 (1958).
[4] U. Bonse and M. Hart, *Appl. Phys. Letters* **6,** 155 (1965).
[5] A. R. Lang, *Acta Cryst.* **12,** 249 (1959).
[6] H. Hashimoto, M. Mannami, and T. Naiki, *Phil. Trans. Roy. Soc.* **253,** 459 (1961).
[7] R. Gevers, *Phil. Mag.* **7,** 1681 (1962).
[8] N. Kato and A. R. Lang, *Acta Cryst.* **12,** 787 (1959).
[9] A. R. Lang, *J. Appl. Phys.* **30,** 1748 (1959).

MOS CONDUCTANCE TECHNIQUE FOR MEASURING SURFACE STATE PARAMETERS

(SiO_2–Si; E)

E. H. Nicollian and A. Goetzberger
Bell Telephone Laboratories, Incorporated
Murray Hill, New Jersey
(Received 3 September 1965)

Determination of fast surface state parameters from loss in an SiO_2-Si MOS capacitor is discussed in this Letter. The surface state parameters sought are capture cross-sections for holes and electrons and number of surface states per cm^2 per eV.

In a previous paper,[1] variation of equivalent parallel conductance and capacitance of inverted surfaces has been explained. The present Letter deals with the depletion inversion region where current flow is one-dimensional perpendicular to the surface. It is shown that equivalent parallel conductance can be used to determine surface state parameters with greater accuracy than possible from capacitance measurements.

Terman[2] showed that fast surface state capacitance and time constants could be determined from

dispersion of the MOS capacitance. The limitations of this method have been discussed in detail by Zaininger and Warfield.[3] Essentially the difficulty is that surface state capacitance must be extracted from measured capacitance which consists of oxide capacitance, depletion layer capacitance, and surface state capacitance. This difficulty does not apply to the measured conductance because it is directly related to the surface states.

To prove that measured conductance is due only to surface states, it is shown that loss in the oxide and space charge region is negligible. A simple experiment shows that the loss is not in the oxide. In Fig. 1*a*, measured capacitance and equivalent parallel conductance are plotted as functions of field-plate bias before and after temperature aging an unstable oxide. Aging produces a large increase in field in the oxide as seen by the shift of the capacitance curve to higher negative bias. Because the conductance curve has not changed in shape or magnitude, it is independent of field in the oxide. Peak conductance occurs at the same value of capacitance before and after aging. Therefore, conductance is a function of surface potential as is capacitance. Estimated loss in the space charge region is negligible unless the silicon contains a very high density of recombination centers. This is seen experimentally. Figure 1*b* shows measured conductance curves for an oxide grown in dry oxygen and one grown in steam, all other parameters being the same. The oxide can be cycled from one state to the other by heat treatment between 200°C and 400°C in various ambients. Because the magnitude of conductance for the dry oxide is considerably greater than for the wet oxide and can be reversibly cycled at low temperatures, the loss cannot be in the space charge region. The fact that the loss is neither in the oxide nor space charge region means that is is an interface effect.

In *p*-type silicon, the primary properties of the conductance are: peak conductance increases by about two orders of magnitude from 1 kc/sec to 100 kc/sec and shifts to a higher negative bias. Extraction of surface state parameters from these properties is best understood in terms of an equivalent circuit. The equivalent circuit shown in Fig. 2a is a simplified version of the one given by Lehovec and Slobodskoy.[4] In Fig. 2a, only interaction between surface states and the majority carrier band is taken into account. This is justified because measurements are restricted to frequencies above 100 cps and it has been shown[5,6] that these frequencies are too high for minority carriers to follow.

The time constant, τ, of the surface states is $R_S C_S$. In terms of Shockley-Read parameters,[7] it becomes $\tau = (\bar{v}\,\sigma p_S)^{-1}$ where $\bar{v}$ is the average thermal velocity of a majority carrier, σ its capture cross-section, and

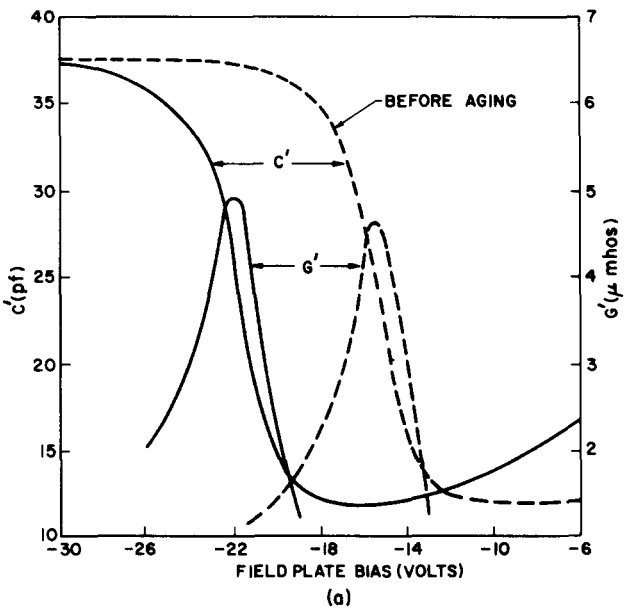

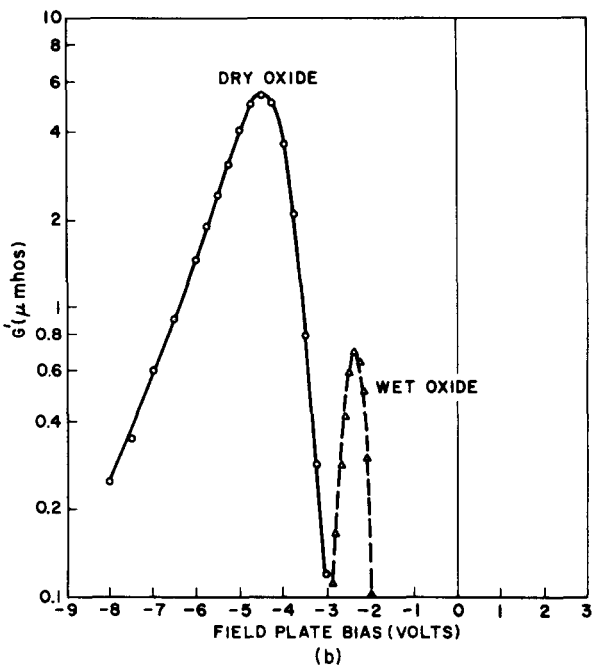

Fig. 1. (a) Measured capacitance and equivalent parallel conductance as functions of field-plate bias before and after temperature aging at 150°C. Field-plate diam is 3.8×10^{-2} cm, silicon resistivity 50 Ω-cm, *p*-type, oxide thickness 1200 Å, and frequency 100 kc/sec.

(b) Measured equivalent parallel conductance as a function of field-plate bias for a dry and a wet oxide. Field-plate diam is 3.8×10^{-2} cm, silicon resistivity 2 Ω-cm, *p*-type, oxide thickness 600 Å, and frequency 100 kc/sec.

p_S majority carrier density at the surface. This equation has been modified from that in ref. 7 for the case of a continuum of states where σ is independent of surface state energy. In terms of surface potential, τ becomes $(\bar{v}\ \sigma p_i)^{-1} \exp(-U_s)$ where n_i is intrinsic carrier concentration and U_s the potential difference between mid-gap and Fermi level at the surface in units of kT/q.

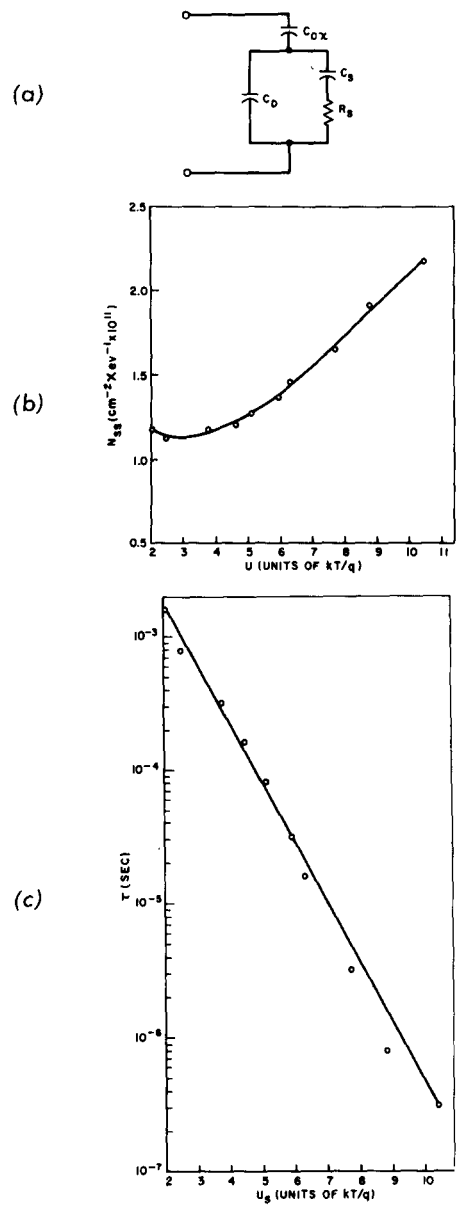

Fig. 2. (a) Simplified equivalent circuit of MOS capacitor. C_{ox} is oxide capacitance, C_D depletion layer capacitance, C_S surface state capacitance, and R_S surface state capture resistance.

(b) Surface state density as a function of energy in the band gap for a 1-Ω-cm, *p*-type, 10 μ thick epitaxial layer. Mid-gap is at $U = 0$ and flat bands at $U = 14$.

(c) Surface state time constant as a function of surface potential. Mid-gap is at $U_s = 0$ and flat bands at $U_s = 14$.

Capacitance of the network consisting of C_s, R_s, and C_D obtained by correcting for C_{ox} (see ref. 1) is:

$$C = C_D + \frac{C_S}{1 + \omega^2\tau^2} \tag{1}$$

where ω is angular frequency, C_S and τ cannot be extracted from this capacitance without knowing C_D. Equivalent parallel conductance, G, of the corrected network, however, depends only on the surface state branch of the equivalent circuit. Thus,

$$G/\omega = \frac{C_S\omega\tau}{1 + \omega^2\tau^2} \tag{2}$$

G/ω goes through a maximum when $\omega\tau = 1$ which gives τ. The value of G/ω at the maximum is $C_S/2$.

Meaningful results can be obtained on oxides which are stable and reproducible. Bias steam grown oxides[8] on *p*-type silicon were investigated. This oxide is grown on a 10-μ thick, 1-Ω-cm, freshly prepared, epitaxial layer of *p*-type silicon to minimize series resistance and provide a clean initial surface. Equivalent parallel conductance in the high accumulation range is very low and fully accounted for by series resistance. There is no influence on conductance by the choice of metal used for the field plate.

Figure 2*b* is obtained by varying surface potential with frequency as parameter. C_S is calculated from the peak of G/ω where $\omega\tau = 1$. Surface state density, N_{SS}, is C_S/qA, where q is the electronic charge and A the field plate area. This relation is applicable for a slowly varying density of surface states vs energy. For a discrete surface state level, C_S/qA would have to be multiplied by a Fermi factor. The results of this investigation clearly point to a continuous distribution confirming earlier MOS work. The range covered in Fig. 2*b* is about a quarter of the energy gap.

Figure 2*c* shows the variation of τ with surface potential. Values of τ are obtained by varying surface potential with frequency as parameter and using the condition $\omega\tau = 1$. Surface potential is obtained *directly* by a low frequency capacitance technique developed by C. N. Berglund.[9]

The experimental points fit the Shockley-Read relation quite well. This fit means there is a *true* continuum of states and σ is constant within the accuracy of measurement. Calculated σ for holes, using $\bar{v} = 10^7$ cm/sec is about 5.4×10^{-16} cm^2.

Dispersion in the surface state branch of the equivalent circuit is best found by measuring G/ω as a function of frequency with field-plate bias as parameter. The experimental curves cannot be

fitted with a single time constant indicating dispersion. It is presently believed that broadening is due to local fluctuations of surface potential.

Values of N_{SS} and τ obtained by varying frequency with surface potential as parameter are consistent with values of these quantities obtained by varying surface potential with frequency as parameter. In view of dispersion in the surface state branch, these are the *dominant* surface state densities and time constants.

Major results of this work using bias grown oxides on p-type silicon are: there is a continuum of hole capturing states with a density around 10^{11} cm^{-2} eV^{-1}, capture cross-section for holes is about 5.4×10^{-16} cm^2, and there is a distribution of time constants at each value of applied bias.

[1]E. H. Nicollian and A. Goetzberger, *IEEE Trans. on Electron Devices* Vol. ED-12, March 1965, p. 108.
[2]I. M. Terman, *Solid-State Electron.* **5,** 285 (1962).
[3]K. H. Zaininger and G. Warfield, *IEEE Trans. on Electron Devices* Vol. ED-12, April 1965.
[4]K. Lehovec, and A. Slobodskoy, *Solid-State Electron.* **7,** 59 (1964).
[5]S. R. Hofstein and G. Warfield, *Solid-State Electron* **8,** 321 (1965).
[6]A. S. Grove, E. H. Snow, B. E. Deal, and C. T. Sah, *J. Appl. Phys.* **35,** 2458 (1964).
[7]A. E. Iunovich, *Sov. Phys.-Tech. Phys.* **3,** 646 (1958).
[8]A. Goetzberger, *J. Electrochem. Soc.* **112,** 150C (July 1965). Full article to be published in *J. Electrochem. Soc.*
[9]C. N. Berglund, to be published.

THE POLARIZATION OF LIGHT FROM Nd^{3+}-GLASS LASERS[1]

(time resolution <1 μsec; E)

Sun Lu and T. A. Rabson
Rice University
Houston, Texas
(Received 22 July 1965; in final form 24 September 1965)

The polarization of the light from a glass laser doped with 2% Nd^{3+} has been measured with a time resolution of less than a microsecond. Although the spiked nature of the output light from optically pumped solid-state lasers is a well-known phenomenon and several theories have been developed which partially explain it,[2] no one has developed a model which gives a complete explanation for the character of the spiking. It is felt that before a satisfactory theory to explain the nature of the spiking phenomenon can be developed, complete measurements of the properties of the light emitted in each spike must be made. Since polarization is one of the fundamental properties of light it is important to know the state of polarization of the light in each spike of the laser output in order to better understand the physical processes which lead to spiking. Although some measurements have been made of the polarization of the light output of ruby lasers, no variation from spike to spike in the polarization of the light was observed and so high time resolution measurements were not needed.[3]

A detailed description of the apparatus used to measure the polarization is given in another paper.[4] In brief, the beam is split into six identical components and an analysis is made using several polarization analyzers, a quarter wave plate, and six photomultiplier detectors. The accuracy of the measurement techniques is about ±5% for the percentage polarization and about ±4° for the direction of polarization. The most serious limitation of the measurement technique used is that no spatial variation in polarization across the cross section of the beam can be measured. In fact, such variations will contribute to the component of beam which is measured as being unpolarized. For this reason the percent polarization reported here can be considered as the lower limit on the percent polarization of the light contained in any subarea of the beam's cross section.

The measurements that have been made using the techniques described above indicate that the polarization of the 1.06-μ light emitted by a 2% Nd^{3+}-doped pulsed laser changes from spike to spike. About two thousand spikes from about 100 pulses have been analyzed, and only general conclusions can be reached. The percentage of polarized light from the laser appears to increase as one goes to lower pumping energies. This is indicated in Fig. 1. This effect could be a result of only a small cross section of the rod actually lasing at low pumping energies whereas several regions may emit light independently at higher energies. However, since measurements were not made of the